

# Regional Climate Effects of Internally and Externally Mixed Aerosols over China

YU Yong<sup>1,2</sup> (于 勇), NIU Shengjie<sup>2</sup> (牛生杰), ZHANG Hua<sup>3\*</sup> (张 华), and WU Ziyue<sup>4</sup> (吴自越)

<sup>1</sup> School of Remote Sensing, Nanjing University of Information Science & Technology, Nanjing 210044

<sup>2</sup> Key Laboratory for Atmospheric Physics and Atmospheric Environment, Nanjing University of Information Science & Technology, Nanjing 210044

<sup>3</sup> Laboratory for Climate Studies, National Climate Center, China Meteorological Administration, Beijing 100081

<sup>4</sup> Meteorology Bureau of Pukou District of Nanjing, Nanjing 211800

(Received March 10, 2012; in final form October 10, 2012)

## ABSTRACT

A regional climate model is employed to simulate the aerosols (dust, sulfate, black carbon, and organic carbon) and their direct effect on the climate over China. The emphasis is on the direct radiative forcing due to the change in mixing state of aerosols. The results show that direct radiative forcing is significantly different between externally and internally mixed aerosols. At the top of the atmosphere (TOA), the radiative forcing of externally mixed aerosols is larger than that of internally mixed ones, especially in the Tarim desert region where the difference is about  $0.7 \text{ W m}^{-2}$ . At the surface, however, the situation becomes opposite, especially in the Sichuan basin where the difference is about  $-1.4 \text{ W m}^{-2}$ . Nonetheless, either externally or internally mixed aerosols in China can result in a significant cooling effect, except for the warming in South China in winter and the slight warming in North China in February. The cooling effect induced by externally mixed aerosols is weaker than that induced by internally mixed aerosols, and this is more obvious in spring and winter than in summer and autumn. In spring and summer, the inhibiting effect of externally mixed aerosols on precipitation is less than that of internally mixed aerosols, whereas in autumn and winter the difference is not obvious.

**Key words:** radiative forcing, internally mixed aerosols, externally mixed aerosols, climate effect

**Citation:** Yu Yong, Niu Shengjie, Zhang Hua, et al., 2013: Regional climate effects of internally and externally mixed aerosols over China. *Acta Meteor. Sinica*, **27**(1), 110–118, doi: 10.1007/s13351-013-0111-1.

## 1. Introduction

The radiative impact of aerosols is one of the largest sources of uncertainty in estimating climate perturbations (Chung et al., 2010; Chung and Seinfeld, 2002; Gu et al., 2006; Cooke et al., 2002; Jacobson, 2000; Kim et al., 2008; Koch, 2001; Schwarz et al., 2008; Stier et al., 2006; Wang, 2004; Zhang et al., 2010; Zhang et al., 2011). Compared to the radiative impact due to well-mixed green-house gases, estimation of the aerosol radiative effect is much more complicated. One reason is that optical properties of aerosols usually change through long-range transport,

and aerosols are not homogeneously mixed in the atmosphere.

Many scientists have investigated the climate impact of aerosols based on the models that treat aerosol as externally mixed, but their assessments appear to be unrealistic (Satheesh et al., 2006). Jacobson (2001a) pointed out that when smaller aerosols accumulate over larger ones, the radiative impact is significantly different compared to that of an external mixture. During the emission, Brownian motion, diffusion, coagulation, condensation, dry or wet deposition, and so on, aerosols are often mixed, to some extent, with other combustion products, such as sulfate

Supported by the National Basic Research and Development (973) Program of China (2011CB403405) and National Science and Technology Support Program of China (2008BAC40B02).

\*Corresponding author: huazhang@cma.gov.cn.

©The Chinese Meteorological Society and Springer-Verlag Berlin Heidelberg 2013

and black carbon (Novakov et al., 1997). When black carbon is coated with organic carbon, the absorptivity of the composite aerosol can be increased (e.g., Fuller et al., 1999; Jacobson, 2001b; Schnaiter et al., 2003). The large heating of the lower atmosphere in response to aerosol absorption may have a substantial influence on atmospheric stability and hence cloud formation over the tropics. The consequent effect on the monsoon has not been understood well. Large heating further enhances the cloud “burn off” as proposed by Ackerman et al. (2000).

Hence, more investigations are urgently needed to study the mixing state of aerosols, which is essential to accurate estimation of the climate impact of aerosols. The treatment of aerosol in a mixed state is particularly important over the Asian region, where natural and anthropogenic aerosols co-exist.

In this paper, regional climate effects of internally and externally mixed aerosols including dust, black carbon, organic carbon, and sulfate over China are investigated based on numerical simulations.

## 2. Model description and method

Aerosols are transported through large-scale circulation and interact closely with cloud and radiative processes. A comprehensive study of aerosol direct climate forcing requires a climate model that incorporates various interactive atmospheric processes. In the following, we study the direct climatic effect of aerosols in China and their impact on regional climatic perturbations by using the Regional Climate Model version 3.0 (RegCM3) developed at the Abdus Salam International Centre for Theoretical Physics (ICTP). The main physical parameterization packages of RegCM3 include the radiative scheme, land surface scheme, planetary boundary layer scheme, cumulus convective scheme, large-scale precipitation scheme, and pressure gradient scheme. The RegCM3 outputs include more than 40 physical quantities of the atmosphere, surface, and radiative variables.

The simulation domain is shown in Fig. 1 along with topography, and the three sub-regions for the comparison of simulated results are also outlined. The

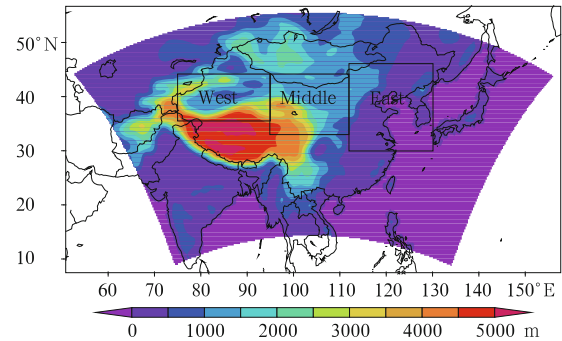


Fig. 1. Model domain and topography (m).

domain is centered at  $34.0^{\circ}\text{N}$ ,  $104.0^{\circ}\text{E}$  under the Lambert map projection, and the horizontal mesh consists of 128 (west-east) and 80 (south-north) grid points with a 60-km resolution, and 18 vertical layers with the model top at 5 hPa. The domain covers the whole China. The model baseline integration was initialized on January 1, 2000, and completed on December 31, 2006. The three sub-regions are: (a) west:  $35.5^{\circ}$ – $44^{\circ}\text{N}$ ,  $75^{\circ}$ – $95^{\circ}\text{E}$ ; (b) middle:  $33^{\circ}$ – $44^{\circ}\text{N}$ ,  $95^{\circ}$ – $112^{\circ}\text{E}$ ; and (c) east:  $30^{\circ}$ – $46^{\circ}\text{N}$ ,  $112^{\circ}$ – $130^{\circ}\text{E}$ , respectively.

The lateral boundary conditions used in the simulation are taken from the NCEP/NCAR reanalysis data for the same period at a horizontal resolution of  $2.5^{\circ}\times 2.5^{\circ}$  at 6-h intervals, and are temporally interpolated with the exponential relaxation method. The weekly optimum interpolation sea surface temperature (OISST) data with a  $1^{\circ}\times 1^{\circ}$  spatial resolution from the Integrated Global Ocean Service System are used. The black carbon, organic carbon, and sulfur dioxide emission rate data are downloaded from the website: <http://users.Ictp.It/pubregcm/RegCM3/>.

The total aerosol radiative forcing can be computed by summing up the radiative forcing of each aerosol species. The result will depend on the assumptions made on how the different aerosol components are mixed together. At one extreme, each aerosol component can be assumed to be physically separated from the other components creating an external mixture of chemically pure modes. At the other extreme, the aerosols can be assumed to be internally mixed as a homogeneous material reflecting the chemical and physical average of all the contributing components. The real mixed state can be expected to lie somewhere

between these two extremes.

The default version of RegCM3 treats aerosol as externally mixed. In this case, all the aerosols are assumed to be spherical so that Mie theory is used to obtain the extinction efficiency of each constituent. The total extinction efficiency and phase function are evaluated by the method of weighted average, for example,

$$K_{\text{ext}}(\lambda) = \frac{\sum_i K_{\text{ext}(i)}(\lambda) f_i}{\sum_i f_i}, \quad (1)$$

where  $K_{\text{ext}}(\lambda)$  is the total extinction efficiency,  $\lambda$  is the wave band, and  $f$  is the mixing ratio. The subscript  $i$  denotes a particular constituent. In this way, it is easily coded to investigate the direct radiative forcing of externally mixed aerosols.

For internally mixed aerosols (core-shell mode) (Vester et al., 2007; Worringen et al., 2008), the calculation is as below,

$$\begin{cases} \gamma_1 = \frac{a^3}{b^3}, \\ \gamma_2 = 1 - \frac{a^3}{b^3}, \end{cases} \quad (2)$$

where  $\gamma_1$  is the volume fraction of a core,  $\gamma_2$  is the volume fraction of its shell,  $a$  is the radius of the core, and  $b$  is the radius of the shell. Since  $\gamma_1$  and  $\gamma_2$  are known, we can obtain the radius  $a$  and  $b$  by solving Eq. (2), and then obtain the two important parameters,  $2\pi a/\lambda$  and  $2\pi b/\lambda$ . These two parameters are the inputs to the core-shell mode algorithm developed by Yang (2003) to calculate the optical properties of a multi-layered sphere (Huang et al., 2007). In this way, the database of optical properties of aerosols is created for internal mixing aerosols and put at the website: [http://climadods.ictp.trieste.it/data/d4/CHEM\\_FB/AERGLOB/optdat.bin](http://climadods.ictp.trieste.it/data/d4/CHEM_FB/AERGLOB/optdat.bin). It is a 6-dimensional optical database named extmix (4, 19, 11, 11, 11, and 11). We can put the database into RegCM3 to consider the internal mixing of aerosols. The first dimensional number “4” represents a class of diameter division, which is the one of dust particles; “19” and “11” in the array represent wave band number and aerosol volume fraction number, respectively. In this study, the spherical

particle is made of two concentric regions, the shell and the core, each with its own uniform refractive index. Note that each of the refractive indices for the shell and core can be averagely determined by aerosols volume fractions.

The purpose of this work is to study the direct radiative forcing and climate response resulting from the assumption of internally and externally mixed aerosols over China. Other effects, such as the first and second indirect forcings, are not considered here. To address the uncertainty in the magnitude of the calculated direct radiative forcing with respect to the mixing state of aerosols, three extreme cases are considered. The first experiment EXTERNAL treats aerosols as externally mixed, and the aerosols include dust, black carbon, organic carbon, and sulfur dioxide. The second experiment INTERNAL treats the aerosols as internally mixed. The last experiment, named CONTROL, considers all the aerosols, but the aerosol radiative heating is not called back to the main program, which means that the model dynamic is not perturbed by aerosols in this case. Note that the distinction between externally and internally mixed cases only pertains to the optical properties of aerosols but not to the physical and chemical properties of the aerosols.

### 3. Simulation results

Figures 2a and 2c show retrieved aerosol optical depth (AOD) using the Earth Observation System Moderate-resolution Imaging Spectroradiometer (EOS/MODIS) data. We can see that major aerosol concentration is located in the Sichuan basin and East China. In comparison, Figs. 2b and 2d give the corresponding simulation results by RegCM3 (CONTROL experiment). It is shown that the model has successfully captured the main distribution characteristics of the AOD, consistent with the observation not only in the AOD areas, but also in the AOD strength. Therefore, we can use this model to make further studies.

#### 3.1 Direct radiative forcing and climatic perturbation of externally mixed aerosols

In this section, we investigate the direct radiative

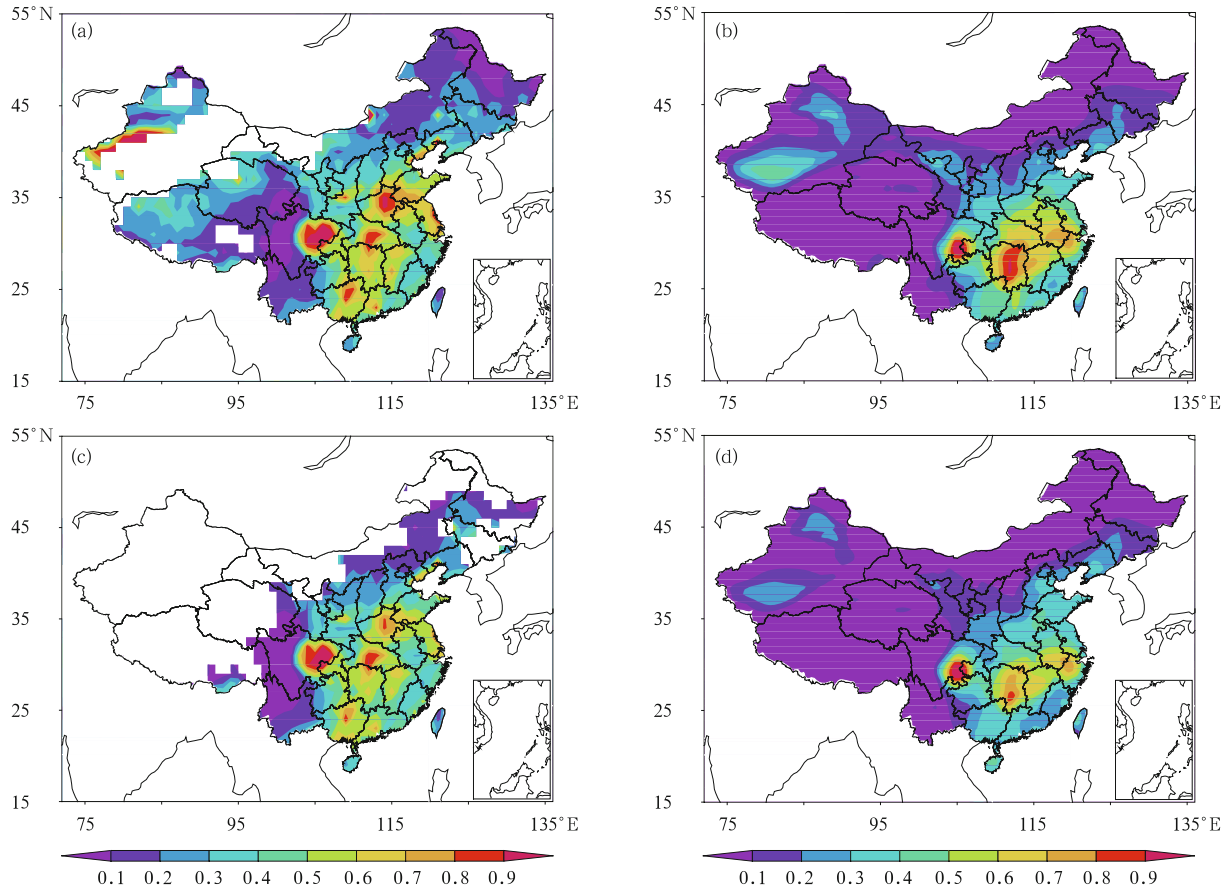


**Fig. 2.** (a, c) Observed and (b, d) simulated mean AOD over China for (a, b) summer and (c, d) winter.

forcing of externally mixed aerosols over China, including dust, sulfate, black carbon and organic carbon, and their climate effect.

Figure 3a shows the simulated direct radiative

forcing of externally mixed aerosols at the surface. The maximum center is located in the Sichuan basin and the second largest value of about  $-18 \text{ W m}^{-2}$  appears in the southern Taklimakan desert, Hunan,

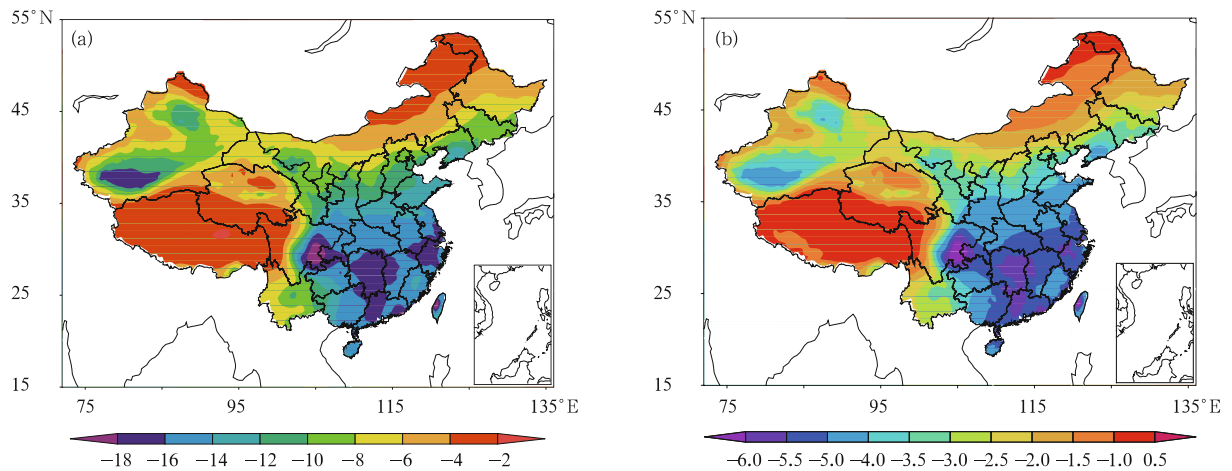


**Fig. 3.** Simulated radiative forcing ( $\text{W m}^{-2}$ ) of externally mixed aerosols at the (a) surface and (b) TOA.

Guangdong, Anhui, and Zhejiang provinces. The whole southeast region is in the high value area. Similarly, in Fig. 3b, the distribution of the forcing at the top of the atmosphere remains mostly the same as that at the surface, though the value is much smaller.

Externally mixed aerosols decrease the precipitation, as shown in Fig. 4a, except in the southern region where the precipitation increases in July. Precipitation tends to decrease in the Sichuan basin and the north region. In the Sichuan basin, the decrease is most obvious in June with values of approximate  $-3.7$  mm day $^{-1}$ , while in the southern region, it is large in early June and September, with values of nearly  $-1.7$  and  $-2.4$  mm day $^{-1}$ , respectively.

The surface air temperature response due to externally mixed aerosols is shown in Fig. 4b. The externally mixed aerosols have a significant cooling effect, except the warming in the south in winter and the slight warming in the northern region in February. In the Sichuan basin, the maximum cooling effect reaches nearly  $-0.38$  and  $-0.55^{\circ}\text{C}$  in early March and early August. In the south region, the surface air temperature curve is V-shaped. From the last 10 days of September to April of the next year, the warming effect becomes more significant. Then, the cooling effect become stronger gradually from the last 10 days of March to the beginning of July, and weakened from the beginning of July to the first 20 days of September.

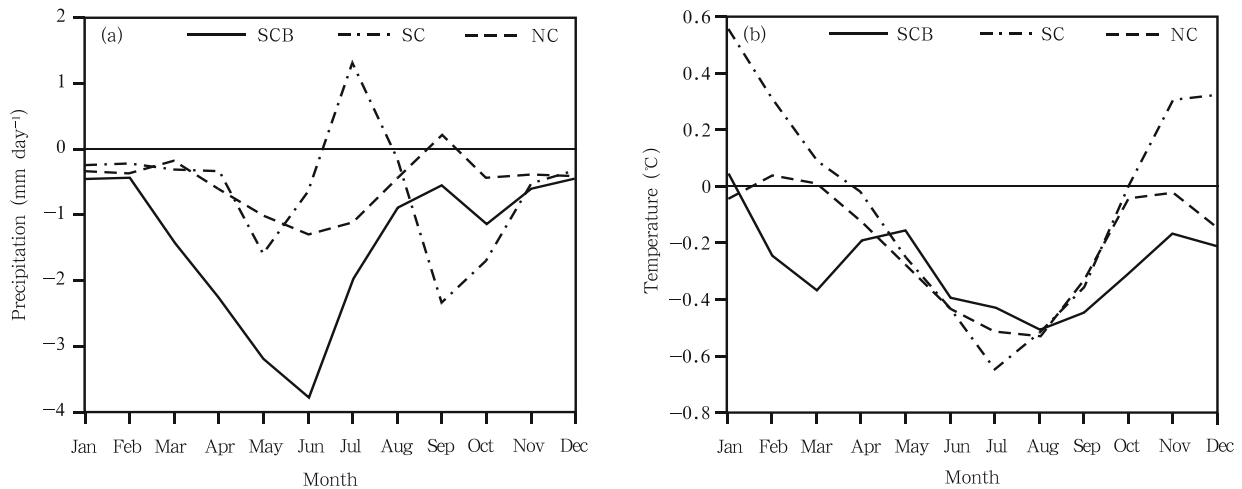


**Fig. 4.** Difference in (a) precipitation and (b) surface air temperature between EXTERNAL and CONTROL over the Sichuan basin (SCB), South China (SC), and North China (NC).

### 3.2 Direct radiative forcing of internally mixed aerosols

The spatial distribution and values of direct radiative forcing derived from internally mixed aerosols are very different from those of externally mixed aerosols. Figure 5a gives simulated radiative forcing of internally mixed aerosols at the surface, with the maximum value of near  $-20$  W m $^{-2}$  located at the southern Taklimakan desert. The entire eastern and southern regions, Xinjiang, Badan Jaran desert and Tengger desert region, and the Sichuan basin are high value areas ( $-10$  W m $^{-2}$  above). The northern Inner Mongolia region and the Qinghai-Tibetan Plateau are minimum value areas (about  $-2$  W m $^{-2}$ ).

Figure 5b shows the direct radiative forcing at the TOA caused by the internally mixed aerosols. The maximum of about  $-5$  W m $^{-2}$  is located in the Sichuan basin, Jiangxi and Zhejiang provinces, while the minimum value lies over the Tibetan Plateau with only  $-0.5$  W m $^{-2}$ .

### 3.3 Difference in climatic effect between the externally and internally mixed cases

At the TOA, as shown in Fig. 6a, the radiative forcing of externally mixed aerosols is stronger than that of the internally mixed, most obvious at the Tarim desert, reaching nearly  $0.7$  W m $^{-2}$ . At the

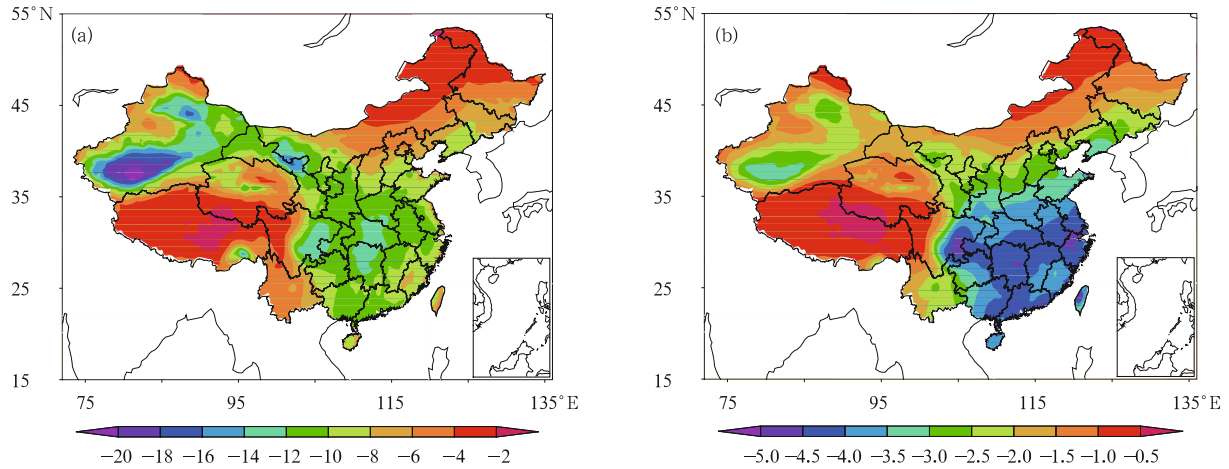


**Fig. 5.** Simulated radiative forcing ( $\text{W m}^{-2}$ ) of internally mixed aerosols at the (a) surface and (b) TOA.

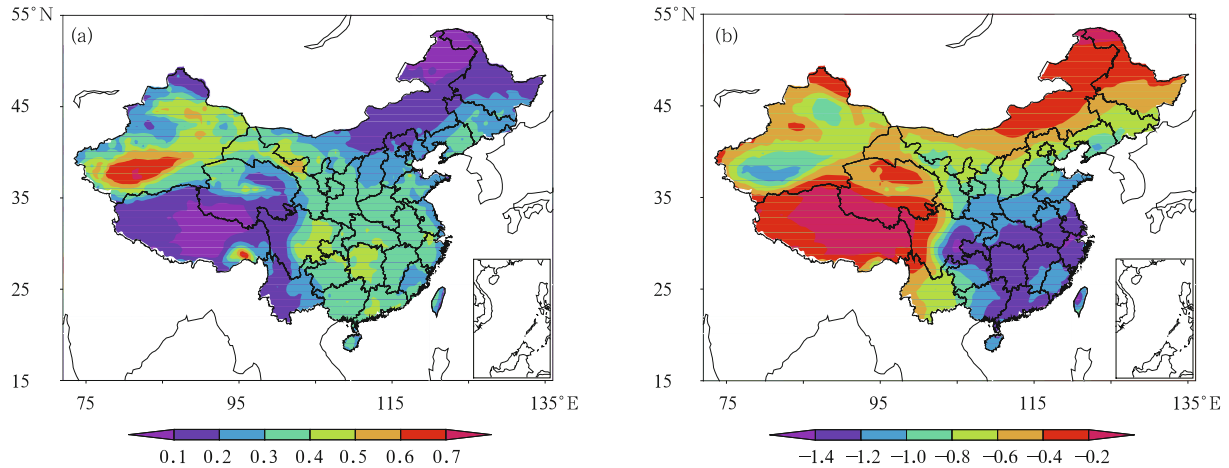


**Fig. 6.** Distributions of the simulated difference of radiative forcing ( $\text{W m}^{-2}$ ) between EXTERNAL and INTERNAL at the (a) TOA and (b) surface.

surface (Fig. 6b), the radiative forcing of externally mixed aerosols is weaker than that of the internally mixed, with the biggest difference of up to  $-1.4 \text{ W m}^{-2}$  in the Sichuan basin, while the difference is the smallest over the Tibetan Plateau, only  $-0.2 \text{ W m}^{-2}$ , because of the low aerosol concentration over the plateau.

In both the externally and internally mixed cases, surface air temperature and precipitation decrease. Figure 7 shows distributions of the simulated difference in surface air temperature between EXTERNAL and INTERNAL experiments, which are mostly positive, indicating that the cooling effect of externally mixed aerosols is less than that of the internally mixed aerosols. The mixing state of aerosols has affected sur-

face air temperature more apparently in spring and winter than in autumn and summer. Especially in spring, the cooling effect of externally mixed aerosols greatly exceeds the internally mixed aerosols by almost  $3.5^\circ\text{C}$ , while this difference is indistinct in summer and autumn ( $< 0.5^\circ\text{C}$ ) and in winter ( $< 1.5^\circ\text{C}$ ).

Based on the long-term data of precipitation and visibility in North China, Duan and Mao (2008) analyzed the interferences of anthropogenic aerosols in North China on the variations of precipitation, and found that aerosols lead to reduction of local precipitation especially in summer. In this paper, we found that the inhibiting effect of aerosols on precipitation changes seasonally, under different mixing states.

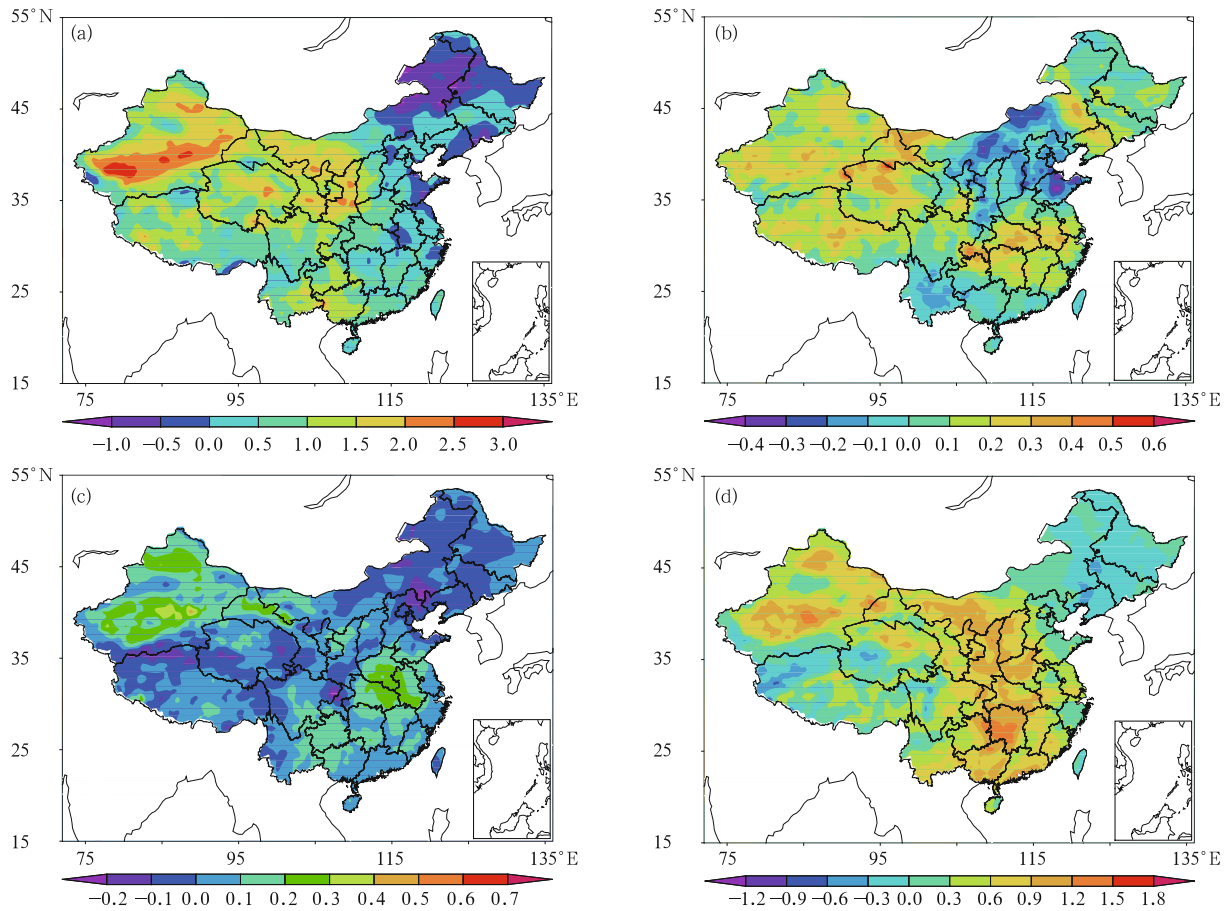


**Fig. 7.** Distributions of the simulated difference of surface air temperature ( $^{\circ}\text{C}$ ) between EXTERNAL and INTERNAL in (a) spring, (b) summer, (c) autumn, and (d) winter.

Figure 8 shows distributions of the simulated difference in precipitation between externally and internally mixed aerosols. The mixing state of aerosols has affected precipitation more apparently in spring and summer than in autumn and winter. The change is largely positive in spring and summer, indicating that the inhibiting effect of externally mixed aerosols on precipitation is less than that of the internally mixed. In autumn and winter, a positive area alternates with a negative area, with respective square area being the same; thus, the mixing state of aerosols has exerted little effect on precipitation in autumn and winter.

#### 4. Summary

In this paper, we investigated the regional climate effects of internally and externally mixed aerosols over

China. Through comparing the direct radiative forcing and surface temperature and precipitation under the influence of the mixing state, we draw the following conclusions.

(1) Both the spatial distribution and the values of direct radiative forcing are significantly different between EXTERNAL and INTERNAL.

(2) Whether externally mixed or internally mixed, aerosols in China resulted in a significant cooling effect, except the warming in South China in winter and the slight warming in North China in February. The cooling effect induced by externally mixed aerosols is weaker than that induced by internally mixed aerosols, which is especially obvious in spring and winter than in summer and fall.

(3) In spring and summer, the inhibiting effect of externally mixed aerosols on precipitation is less than

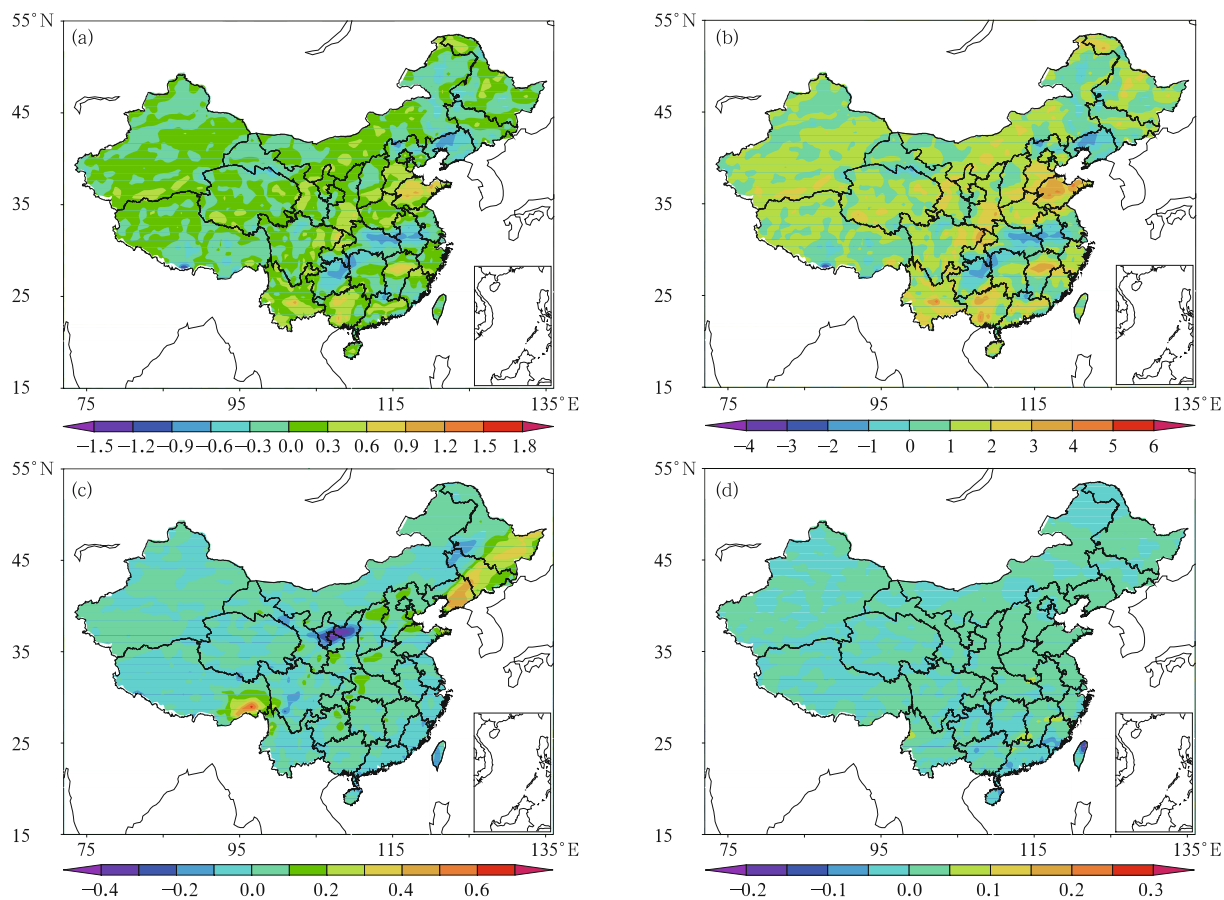


**Fig. 8.** Distributions of the simulated difference of precipitation ( $\text{mm day}^{-1}$ ) between EXTENRAL and INTERNAL in (a) spring, (b) summer, (c) autumn, and (d) winter.

that of internally mixed aerosols, whereas in autumn and winter, the difference is not obvious.

## REFERENCES

- Ackerman, A. S., O. B. Toon, D. E. Stevens, et al., 2000: Reduction of tropical cloudiness by soot. *Science*, **288**, 1042–1047.
- Chung, C. E., V. Ramanathan, G. Carmichael, et al., 2010: Anthropogenic aerosol radiative forcing in Asia derived from regional models with atmospheric and aerosol data assimilation. *Atmos. Chem. Phys.*, **10**, 6007–6024.
- Chung, S. H., and J. H. Seinfeld, 2002: Global distribution and climate forcing of carbonaceous aerosols. *J. Geophys. Res.*, **107**, 4407, doi: 10.1029/2001JD001397.
- Cooke, W. F., V. Ramaswamy, and P. Kasibhatla, 2002: A general circulation model study of the global carbonaceous aerosol distribution. *J. Geophys. Res.*, **107**, 4279, doi: 10.1029/2001JD001274.
- Duan Jing and Mao Jietai, 2008: The effect of aerosols on precipitation in North China. *Chinese Sci. Bull.*, **53**(23), 2947–2955. (in Chinese)
- Fuller, K. A., W. C. Malm, and S. M. Kreidenweis, 1999: Effects of mixing on extinction by carbonaceous particles. *J. Geophys. Res.*, **104**(15), 941–954.
- Gu, Y., K. N. Liou, Y. Xue, et al., 2006: Climatic effects of different aerosol types in China simulated by the UCLA general circulation model. *J. Geophys. Res.*, **111**, D15201, doi: 10.1029/2005JD006312.
- Huang Honglian, Huang Yinbo, Han Yong, et al., 2007: Light extinction properties of marine aerosol particles in internal mixing state. *J. Atmos. Environ. Opt.*, **2**(3), 1066–1070. (in Chinese)
- Jacobson, M. Z., 2000: A physically-based treatment of elemental carbon optics: Implication for global direct forcing of aerosols. *Geophys. Res. Lett.*, **27**(2), 217–220.

- , 2001a: Strong radiative heating due to the mixing state of black carbon in atmospheric aerosols. *Nature*, **409**, 695–697.
- , 2001b: Global direct radiative forcing due to multi-component anthropogenic and natural aerosols. *J. Geophys. Res.*, **106**, 1551–1568.
- Kim, D., C. Wang, A. M. L. Ekman, et al., 2008: Distribution and direct radiative forcing of carbonaceous and sulfate aerosols in an interactive size resolving aerosol-climate model. *J. Geophys. Res.*, **113**, 16309, doi: 10.1029/2007JD009756.
- Koch, D., 2001: The transport and direct radiative forcing of carbonaceous and sulfate aerosols in the GISS GCM. *J. Geophys. Res.*, **106**, 20311–20332.
- Novakov, T., D. A. Hegg, and P. V. Hobbs, 1997: Airborne measurements of carbonaceous aerosols on the east coast of the United States. *J. Geophys. Res.*, **102**, 30023–30030.
- Satheesh, S. K., J. Srinivasan, V. Vinoj, et al., 2006: New directions: How representative are aerosol radiative impact assessments? *Atmos. Environ.*, **40**, 3008–3010.
- Schnaiter, M., H. Horvath, O. Mohler, et al., 2003: UV-VIS-NIR spectral optical properties of soot and soot-containing aerosols. *J. Aerosol Sci.*, **34**(10), 1421–1444.
- Schwarz, J. P., J. R. Spackman, D. W. Fahey, et al., 2008: Coatings and their enhancement of black carbon light absorption in the tropical atmosphere. *J. Geophys. Res.*, **113**, 03203, doi: 10.1029/2007JD009042.
- Stier, P., H. Seinfeld, S. Kinne, et al., 2006: Impact of nonabsorbing anthropogenic aerosols on clear-sky atmosphere absorption. *J. Geophys. Res.*, **111**, 18201, doi: 10.1029/2006JD007147.
- Vester, B. P., M. Ebert, E. B. Barnert, et al., 2007: Composition and mixing state of the urban background aerosol in the Rhein-Main Area (Germany). *Atmos. Environ.*, **41**, 6102–6115.
- Wang, C., 2004: A modeling study on the climate impact of black carbon aerosols. *J. Geophys. Res.*, **109**, doi: 10.1029/2003JD004084.
- Worringen, A., M. Ebert, T. Trautmann, et al., 2008: Optical properties of internally mixed ammonium sulfate and soot particles: A study of individual aerosol particles and ambient aerosol populations. *Appl. Opt.*, **47**(21), 3835–3845.
- Yang, W., 2003: Improved recursive algorithm for light scattering by a multilayered sphere. *Appl. Opt.*, **42**(9), 1710–1720.
- Zhang Hua, Ma Jinghui, and Zheng Youfei, 2010: Modeling study of the global distribution of radiative forcing by dust aerosol. *Acta Meteor. Sinica*, **24**(5), 558–570.
- Zhang Li, Liu Hongnian, and Zhang Ning, 2011: Impacts of internally and externally mixed anthropogenic sulfate. *Acta Meteor. Sinica*, **25**(5), 639–658.